

# Tunable decoherence in the vicinity of a normal metal–superconducting junction

Rodolphe Guyon<sup>a</sup>, Thierry Martin<sup>a</sup> and Gordey B. Lesovik<sup>a,b</sup>

<sup>a</sup>*Centre de Physique Théorique, Université de la Méditerranée, Luminy Case 907, F-13288 Marseille Cedex 9, France*

<sup>b</sup>*L. D. Landau Institute for Theoretical Physics, 117940 Moscow, Russia*

The decoherence rate of a quantum dot coupled to a fluctuating environment described by a normal–metal superconductor junction is considered. The density–density correlator at low frequencies constitutes the kernel which enters the calculation of the phase coherence time. The density fluctuations are connected to the finite frequency current–current correlations in the point contact via the continuity equation. Below and above the gap, at zero temperature the density correlator contains spatial oscillations at half of the Fermi wave length on the normal side. As the bias crosses the superconducting gap, the opening of new scattering channels enhances the decoherence rate dramatically, suggesting the possibility of tuning the decoherence rate in a controllable manner.

## I. INTRODUCTION

The problem of decoherence in mesoscopic systems has remained a central issue for two decades. With the possible advent of quantum computers, it now occupies an even more important role, as the limitations associated with various decoherence mechanisms provide the fundamental working limits of these devices. Proposals for studying decoherence in Aharonov–Bohm (AB) type geometries have been made<sup>1</sup>. Experiments in the last decade have provided information on the phase shift suffered by an electron propagating through a quantum dot<sup>2,3</sup>. These interference experiments show that coherent propagation through a dot is indeed possible. A few years ago, decoherence was introduced artificially in these same AB devices by placing a quantum point contact in the vicinity of the dot<sup>4</sup>. Alternatively, dephasing has been studied experimentally using a phase sensitive double dot detector<sup>5</sup>. Because quantum transport is a stochastic process, current noise or charge fluctuations act as a dissipative environment coupled to the dot, providing decoherence without particle transfer to this environment.

In the present work, the decoherence rate is computed for the situation where the discrete level (the dot) is coupled electrostatically to the fluctuating charges of a normal metal–superconductor junction with an arbitrary bias. In the Andreev regime, at zero temperature, it is expected that the calculation of the decoherence rate is similar to that of a normal metal point contact except that the charge of the carriers is replaced by the Cooper pair charge<sup>6</sup>. This simple analogy fails both at finite temperatures and at voltage biases superior to the superconducting gap. Specifically, in both the Andreev and the sub–gap regime, the decoherence rate depends crucially on the range of the potential which couples the dot to its environment: when this range is lowered below the Fermi wavelength, oscillatory terms in the density–density correlator contribute substantially to the decoherence rate. Even more stunning is the behavior of the decoherence rate as the voltage bias crosses the gap. The opening of new scattering channels accounts for an additional charge noise, and thus provokes a sharp increase in this rate.

In principle, this could allow to tune the system from a “quantum” behavior to a “classical” behavior in a controllable manner.

The computation of the decoherence rate in the present work, which typically involves the calculation of a density–density correlator in the limit of zero frequency, uses as a starting point known results for the finite frequency current noise<sup>7,8</sup>, rather than a direct computation of the density fluctuations. Indeed, the charge fluctuations are directly connected to the current fluctuations using the continuity equation, which holds in second quantized notation, as will be shown below.

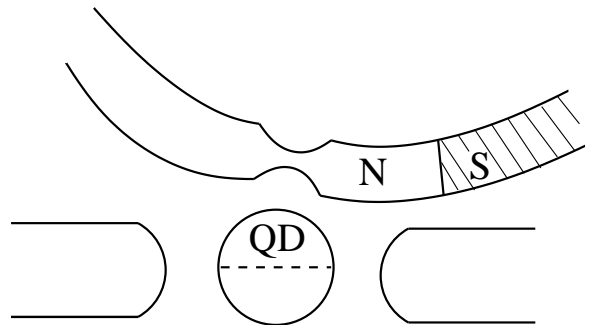


FIG. 1. A quantum dot (QD), which contains a sharp level, is connected to two semi–infinite leads (lower half of the figure). In its vicinity, a fluctuating current flows through a nanoscopic (single channel), normal metal–superconductor junction (upper half). Broadening of the level occurs in the presence of an electrostatic coupling between the dot and the normal side of the NS wire.

Density–density correlations have been recently computed on a formal level<sup>9</sup> in the geometry of Fig. 1. In contrast, here one is interested both in ultra–small junctions and in the transition to the above–gap regime. Moreover, it will be shown that decoherence also occurs for an “ideal” NS junction, the superconducting–normal metal analog of an adiabatic point contact. In all of the above, spatial oscillations of the density–density correlations are shown to occur, and to enter the computation of the decoherence rate. To our knowledge these oscillations have not been described in previous work.

The paper is organized as follows. The model with its basic assumptions is described in section II. The relationship between the phase coherence time and the density–density fluctuations has been established by several authors<sup>10–12</sup> and is reviewed briefly in Appendix A. The main emphasis is put on the analysis of the density–density correlations of the normal–metal superconducting quantum dot, first in the Andreev regime (section IV). Expressions which apply to the case where the disorder potential is smooth – a superconducting adiabatic point contact – are provided. Finally, the case of a bias which is superior to the gap is exposed in section V, and its consequence on the decoherence rate is illustrated numerically using the Blonder Tinkham Klapwijk (BTK) model<sup>13</sup>.

## II. DEPHASING MECHANISM AND NS JUNCTION

A (small) quantum dot, which for practical purposes here is represented by a discrete, sharp energy level, is located in the proximity of a (single channel) normal metal–superconductor (NS) junction (Fig. 1). The dot is connected to two semi–infinite leads, and can in principle be part of an interferometer such as the ones studied in Refs.<sup>4,5</sup>. The dot is coupled by Coulomb forces to the fluctuating charges located in a NS point contact (SPC). To be specific, it is assumed that the electrostatic coupling is restricted to the normal side of the junction, as the dephasing mechanism is expected to be more efficient when the bias voltage on the NS wire is below the superconducting gap.

The system is described by a Hamiltonian which characterized the dot, the NS junction and the coupling between the two:

$$H_C = c^\dagger c \int dx U(x) \psi^\dagger(x) \psi(x) \quad (1)$$

where  $\psi(x)$  and  $c$  ( $\psi^\dagger(x)$  and  $c^\dagger$ ) are fermion creation and annihilation operators in the NS junction and in the dot. The potential  $U(x)$  depends on the location of the charges in the NS junction. While it originates from long range Coulomb forces, in practical situations it is screened by the surrounding metallic gates. Later on, different ranges will be specified for  $U(x)$  in order to observe their consequence on the decoherence rate.

The “standard” procedure<sup>10,11</sup> for computing the decoherence rate  $\tau_\phi^{-1}$  is to identify an exponential decay in time of the dot electron Greens function. Even though there is no electron leak from the dot to the NS junction, the level in the dot acquires a finite width due to the coupling with the fluctuations in the junction. The dot Greens function thus acquires a non–oscillatory component:

$$G(t) = \langle T[c(t)c^\dagger(0)] \rangle_{NS} \propto e^{-t/\tau_\phi} e^{-i\epsilon_0 t/\hbar} \quad (2)$$

where  $\tau_\phi$  is the decoherence time, and the bracket notation  $\langle \rangle_{NS}$  implies that an average over the NS environment has been taken. The following result for the decoherence rate neglects the back–effect of the dot on the NS junction:

$$\frac{1}{\tau_\phi} = \frac{1}{\hbar^2} \int_{-\infty}^{+\infty} dt K(t) \quad (3)$$

with the Kernel defined as:

$$K(t) = \frac{1}{2} \int dx_1 \int dx_2 U(x_1) U(x_2) \times \langle \langle \rho(x_1, t) \rho(x_2, 0) + \rho(x_2, 0) \rho(x_1, t) \rangle \rangle \quad (4)$$

where the notation  $\langle \langle \rangle \rangle$  means that the average densities have been subtracted.

The main issue to compute this rate is to specify the density–density correlator using the property that electrons and holes on the normal side, and possibly quasi–particles on the superconducting side, are scattered at the NS junction. The scattering matrix specifies the amplitudes of the transmitted/reflected particles. It allows to give the asymptotic behavior of the electron and hole wave functions away from the junction<sup>7,14,15</sup>. Here, the notations of previous work<sup>8</sup> are used for convenience.

On the normal side of the NS point contact, the electron and hole wave functions associated with a particle  $\alpha = e, h$  which originates from side  $j = N, S$  are given by:

$$u_{j,\alpha}(x, t) \simeq \frac{\delta_{1j} \delta_{\alpha e}}{(hv_+)^{1/2}} (e^{ik_+x} + s_{Nj ee} e^{-ik_+x}) + \frac{\delta_{\alpha h}}{(hv_+)^{1/2}} s_{Nj eh} e^{-ik_+x} \quad (5)$$

$$v_{j,\alpha}(x, t) \simeq \frac{\delta_{1j} \delta_{\alpha h}}{(hv_-)^{1/2}} (e^{-ik_-x} + s_{Nj hh} e^{ik_-x}) + \frac{\delta_{\alpha e}}{(hv_-)^{1/2}} s_{Nj he} e^{ik_-x} \quad (6)$$

where the electron and hole momenta are specified by  $k_\pm = \sqrt{2m(\mu_S \pm \epsilon)}/\hbar$ , with  $\mu_S$  the chemical potential of the superconductor, which assumed to be large compared to both the gap  $\Delta$  and the bias  $eV$ .  $s_{ij\alpha\beta}$  is the amplitude for a particle of type  $\beta = e, h$  which is incident from side  $j$  to be scattered as a particle of type  $\alpha = e, h$  in reservoir  $i$ . When discussing the Andreev regime, both electrons and holes are incident only from the normal side, and the indices  $i, j = N$  will therefore be dropped in sections III and IV, but will be restored in section V.

Finally, the electron/hole distribution function on the normal side are given by:  $f_{Ne,h} = \{1 + \exp[(\epsilon \mp eV)/k_B \Theta]\}^{-1}$  while on the superconducting side, incident holes and electrons have the same distribution function, with  $V = 0$ .

### III. CURRENT AND DENSITY FLUCTUATIONS

As described before<sup>7</sup>, the statistical average of the current–current operator is obtained by performing the Bogolubov transformation<sup>16</sup> on the current operator. In the past, it was for the most part computed at equal locations in connection with the current noise across the NS junction. For the decoherence time, it is necessary to keep the two locations  $x_1$  and  $x_2$  separate. However, as the current correlators in Refs.<sup>7,8</sup> are expressed with separate time arguments  $t_1$  and  $t_2$ , the generalization to separate spatial arguments is straightforward:

$$\begin{aligned} \langle\langle I(x_1, t_1) I(x_2, t_2) \rangle\rangle &= \frac{e^2 \hbar^2}{2m^2} \sum_{\tilde{\alpha}, \tilde{\beta}} \int_0^{+\infty} \int_0^{+\infty} d\varepsilon d\varepsilon' \left\{ \right. \\ & f_{\tilde{\alpha}}(\varepsilon)(1 - f_{\tilde{\beta}}(\varepsilon')) e^{i(\varepsilon' - \varepsilon)(t_2 - t_1)/\hbar} \\ & \quad \times [(u_{\tilde{\beta}} \overset{\leftrightarrow}{\partial} u_{\tilde{\alpha}}^*)_{t_1, x_1} + (v_{\tilde{\beta}} \overset{\leftrightarrow}{\partial} v_{\tilde{\alpha}}^*)_{t_1, x_1}] \\ & \quad \times [(u_{\tilde{\beta}}^* \overset{\leftrightarrow}{\partial} u_{\tilde{\alpha}})_{t_2, x_2} + (v_{\tilde{\beta}}^* \overset{\leftrightarrow}{\partial} v_{\tilde{\alpha}})_{t_2, x_2}] \\ & + f_{\tilde{\alpha}}(\varepsilon) f_{\tilde{\beta}}(\varepsilon') e^{-i(\varepsilon + \varepsilon')(t_2 - t_1)/\hbar} \\ & \quad \times (u_{\tilde{\beta}}^* \overset{\leftrightarrow}{\partial} v_{\tilde{\alpha}}^*)_{t_1, x_1} [(u_{\tilde{\alpha}} \overset{\leftrightarrow}{\partial} v_{\tilde{\beta}})_{t_2, x_2} + (u_{\tilde{\beta}} \overset{\leftrightarrow}{\partial} v_{\tilde{\alpha}})_{t_2, x_2}] \\ & + (1 - f_{\tilde{\alpha}}(\varepsilon))(1 - f_{\tilde{\beta}}(\varepsilon')) e^{i(\varepsilon + \varepsilon')(t_2 - t_1)/\hbar} \\ & \quad \times [(u_{\tilde{\alpha}} \overset{\leftrightarrow}{\partial} v_{\tilde{\beta}})_{t_1, x_1} + (u_{\tilde{\beta}} \overset{\leftrightarrow}{\partial} v_{\tilde{\alpha}})_{t_1, x_1}] (u_{\tilde{\beta}}^* \overset{\leftrightarrow}{\partial} v_{\tilde{\alpha}}^*)_{t_2, x_2} \left. \right\}, \end{aligned} \quad (7)$$

where  $\tilde{\alpha} = (\alpha, i)$  is a short hand notation combining the reservoir from which the particle, electron or hole, is incident. Eq. (7) constitutes the starting point for computing both finite frequency noise and the zero frequency noise in the presence of a local harmonic perturbation, such as in the Non Stationary AB effect in NS junctions<sup>7</sup> which was recently detected experimentally<sup>6</sup>. Here it constitutes the starting point for the computation of the density–density correlator, and it is valid both in the Andreev regime and above gap, provided that the proper distribution functions are specified on the superconducting side.

The continuity equation allows to relate the current operator to the density operator as it holds in second quantized form:

$$\rho(x, \omega) = \frac{1}{i\omega} \overleftrightarrow{\nabla} \cdot \overleftrightarrow{\mathcal{J}}(x, \omega) \quad (8)$$

This allows to write a connection formula between the nonlocal current noise correlator and the density–density correlator at finite frequency:

$$\begin{aligned} \langle\langle \rho(x_1, \omega) \rho(x_2, -\omega) \rangle\rangle &= \int_{-\infty}^{+\infty} \frac{dt}{\omega^2} e^{i\omega t} \\ & \quad \times \partial_{x_1} \partial_{x_2} \langle\langle I(0) I(t) \rangle\rangle \end{aligned} \quad (9)$$

Here the  $\omega = 0$  density–density correlations will be needed. Taking the derivative with respect to the positions, the  $\omega^2$  term in the denominator is canceled, for all bias regimes, giving a finite contribution to the density fluctuations.

### IV. DENSITY CORRELATOR IN THE ANDREEV REGIME

In the Andreev regime, there are only two types of particles (electrons and holes), so the current–current correlator at finite temperatures and bias takes the form:

$$\begin{aligned} \langle\langle I(x_1, t_1) I(x_2, t_2) \rangle\rangle_A &= \frac{e^2 \hbar^2}{2m^2} \int_0^{+\infty} \int_0^{+\infty} d\varepsilon d\varepsilon' \left\{ \right. \\ & f_e(\varepsilon)(1 - f_h(\varepsilon')) e^{i(\varepsilon' - \varepsilon)(t_2 - t_1)/\hbar} \\ & \quad \times [(u_h \overset{\leftrightarrow}{\partial} u_e^*)_{t_1, x_1} + (v_h \overset{\leftrightarrow}{\partial} v_e^*)_{t_1, x_1}] \\ & \quad \times [(u_h^* \overset{\leftrightarrow}{\partial} u_e)_{t_2, x_2} + (v_h^* \overset{\leftrightarrow}{\partial} v_e)_{t_2, x_2}] \\ & + f_h(\varepsilon)(1 - f_e(\varepsilon')) e^{i(\varepsilon' - \varepsilon)(t_2 - t_1)/\hbar} \\ & \quad \times [(u_e \overset{\leftrightarrow}{\partial} u_h^*)_{t_1, x_1} + (v_e \overset{\leftrightarrow}{\partial} v_h^*)_{t_1, x_1}] \\ & \quad \times [(u_e^* \overset{\leftrightarrow}{\partial} u_h)_{t_2, x_2} + (v_e^* \overset{\leftrightarrow}{\partial} v_h)_{t_2, x_2}] \\ & + f_e(\varepsilon) f_h(\varepsilon') e^{-i(\varepsilon + \varepsilon')(t_2 - t_1)/\hbar} \\ & \quad \times (u_h^* \overset{\leftrightarrow}{\partial} v_e^*)_{t_1, x_1} [(u_e \overset{\leftrightarrow}{\partial} v_h)_{t_2, x_2} + (u_h \overset{\leftrightarrow}{\partial} v_e)_{t_2, x_2}] \\ & + f_h(\varepsilon) f_e(\varepsilon') e^{-i(\varepsilon + \varepsilon')(t_2 - t_1)/\hbar} \\ & \quad \times (u_e^* \overset{\leftrightarrow}{\partial} v_h^*)_{t_1, x_1} [(u_h \overset{\leftrightarrow}{\partial} v_e)_{t_2, x_2} + (u_e \overset{\leftrightarrow}{\partial} v_h)_{t_2, x_2}] \\ & + (1 - f_e(\varepsilon))(1 - f_h(\varepsilon')) e^{i(\varepsilon + \varepsilon')(t_2 - t_1)/\hbar} \\ & \quad \times [(u_e \overset{\leftrightarrow}{\partial} v_h)_{t_1, x_1} + (u_h \overset{\leftrightarrow}{\partial} v_e)_{t_1, x_1}] (u_h^* \overset{\leftrightarrow}{\partial} v_e^*)_{t_2, x_2} \\ & + (1 - f_h(\varepsilon))(1 - f_e(\varepsilon')) e^{i(\varepsilon + \varepsilon')(t_2 - t_1)/\hbar} \\ & \quad \times [(u_h \overset{\leftrightarrow}{\partial} v_e)_{t_1, x_1} + (u_e \overset{\leftrightarrow}{\partial} v_h)_{t_1, x_1}] (u_e^* \overset{\leftrightarrow}{\partial} v_h^*)_{t_2, x_2} \left. \right\} \end{aligned} \quad (10)$$

To proceed, one makes use of the unitarity of the scattering matrix, combined with the time reversal symmetry of electrons and holes in the Andreev regime (energy dependence of scattering coefficients neglected):  $s_{he}^* = -s_{eh}$  and  $s_{ee}^* = s_{hh}$ . Taking the Fourier transform of the current–current correlator, the following relation between the incoming and the scattered wave numbers is obtained:

$$k_{\pm}^2 - k'_{\pm}^2 = \pm \frac{2m}{\hbar} \omega \quad (11)$$

Moreover, the standard simplifications are made ( $\mu_S \gg \omega$ ): once the spatial derivatives are taken and the  $\omega^2$  proportionality in  $\partial_{x_1} \partial_{x_2} \langle\langle I(x_1, t_1) I(x_2, t_2) \rangle\rangle$  is identified, the wave vectors of electrons and holes are assumed to be equal to  $k_F$ .

The density correlator in the Andreev regime becomes:

$$\begin{aligned}
\langle\langle\rho(x_1,\omega)\rho(x_2,-\omega)\rangle\rangle_A &= \frac{e^2}{2\pi^2\hbar v_F^2} \int_0^{+\infty} d\epsilon \left\{ \right. \\
& f_e(\epsilon)(1-f_h(\epsilon-\omega))\Theta(\epsilon-\omega) \\
& \times 4|s_{eh}|^2[|s_{ee}|^2 + s_{ee}^*e^{2ik_Fx_2} + s_{ee}e^{-2ik_Fx_1} + e^{2ik_F(x_2-x_1)}] \\
& + f_h(\epsilon)(1-f_e(\epsilon-\omega))\Theta(\epsilon-\omega) \\
& \times 4|s_{eh}|^2[|s_{ee}|^2 + s_{ee}^*e^{2ik_Fx_1} + s_{ee}e^{-2ik_Fx_2} + e^{2ik_F(x_1-x_2)}] \\
& - f_e(\epsilon)f_h(-\epsilon+\omega)\Theta(-\epsilon+\omega) \\
& \times |s_{eh}|^2\{1-(|s_{eh}|^2 - s_{ee}s_{hh}) + s_{ee}e^{-2ik_Fx_2} + s_{hh}e^{2ik_Fx_2}\} \\
& + f_h(\epsilon)f_e(-\epsilon+\omega)\Theta(-\epsilon+\omega) \\
& \times \left[ 2|s_{ee}|^2\{|s_{ee}|^2 + 1 + s_{ee}(e^{-2ik_Fx_1} + 1/2e^{-2ik_Fx_2}) \right. \\
& \quad + s_{ee}^*(e^{2ik_Fx_1} + 1/2e^{2ik_Fx_2}) + \cos(2k_F(x_2-x_1))\} \\
& \quad + s_{ee}^*e^{2ik_Fx_2}(1 + s_{ee}^*e^{2ik_Fx_1}) \\
& \quad \left. + s_{ee}e^{-2ik_Fx_2}(1 + s_{ee}e^{-2ik_Fx_1}) \right] \left. \right\}
\end{aligned} \tag{12}$$

Further assuming that the temperature  $k_B\Theta < \Delta$ , and neglecting the energy dependence of the scattering matrix coefficients, the thermal integrations are performed in Appendix B.

At zero temperature ( $\omega > 0$ ) the only interval which survives is the one specified by the Fermi functions  $f_e(\epsilon)(1-f_h(\epsilon-\omega))$  (first term in Eq. (12)). At low frequencies, and  $k_B\Theta = 0$ , the double integral in energy is  $eV$  and the correlator becomes:

$$\begin{aligned}
\langle\langle\rho(x_1,\omega)\rho(x_2,-\omega)\rangle\rangle_{A,\omega=0} &= \frac{2e^3V|s_{eh}|^2}{\pi^2\hbar v_F^2} \\
& \times [ |s_{ee}|^2 + s_{ee}^*e^{2ik_Fx_2} + s_{ee}e^{-2ik_Fx_1} + e^{2ik_F(x_2-x_1)} ]
\end{aligned} \tag{13}$$

Note the remarkable fact that the low frequency density–density correlator has an oscillatory spatial dependence with wavelength  $\lambda_F/2$ . These oscillatory terms give a significant contribution to the kernel of Eq. (4) when the envelope function  $U(x)$  is short ranged. Together with the above approximations, the decoherence rate in the Andreev regime can be expressed in terms of the Fourier components  $\tilde{U}(q)$  of the envelope potential at  $q = 0$  and at  $q = \pm 2k_F$ :

$$\begin{aligned}
\frac{1}{\tau_\Phi^A} &= \lim_{\omega \rightarrow 0} \frac{e^2}{\hbar^3 v_F^2} \int_0^{+\infty} d\epsilon f_e(\epsilon)(1-f_h(\epsilon-\omega))\Theta(\epsilon-\omega) \\
& \times [s_{he}^*(s'_{hh}\tilde{U}(0) + \tilde{U}(-2k_F)) \\
& \quad - s'_{eh}(s_{he}^*\tilde{U}(0) + \tilde{U}(-2k_F))] \\
& \times [s_{he}(s'_{hh}\tilde{U}(0) + \tilde{U}(2k_F)) \\
& \quad - s'_{eh}(s_{ee}\tilde{U}(0) + \tilde{U}(2k_F))],
\end{aligned} \tag{14}$$

where prime denotes quantities evaluated at  $\epsilon - \omega$ .

The case of a superconducting adiabatic point contact (SAPC) is now considered momentarily, to highlight

the different role played by charge and current fluctuations for the decoherence rate. This constitutes the NS analog of the adiabatic point contact studied in Ref.<sup>17</sup>. This situation assumes a sharp NS interface with perfect Andreev reflection, adjacent to a scalar potential on the normal side which varies slowly on the scale of the Fermi wave length. While the Andreev reflection processes have a unit probability, it is necessary to take into account the dependence of the electron and hole wave function amplitude on the normal side due to the smooth disorder potential following a quasi–classical/WKB approximation. For simplicity, here only results at zero temperature, in the Andreev regime are presented.

Instead of redefining the electron and hole wave function in this limit, it is more convenient to directly substitute the expressions for the semi–classical matrix elements in the density correlator of Eq. (12):  $|s_{he}|^2 = 1$  and  $s_{ee} = s_{hh} = 0$ . The wave numbers of electrons and holes, which now have acquired a spatial dependence, still satisfy the relationships of Eq. (11).

For the SAPC, the only contribution which survives is the one which is directly proportional to the Andreev reflection probability:

$$\begin{aligned}
\langle\langle\rho(x_1,\omega)\rho(x_2,-\omega)\rangle\rangle_{WKB} &= \\
& \frac{16e^2}{\hbar^2} \int_0^\infty d\epsilon \frac{f_e(\epsilon)(1-f_h(\epsilon-\omega))}{\sqrt{v_+(x_1)v_-(x_2)}} \\
& \times \frac{\exp\left[\int_{x_1}^{x_2} i(k'(x) + k(x))dx\right]}{\sqrt{(v'_+(x_1) + v_+(x_1))(v'_-(x_2) + v_-(x_2))}}
\end{aligned} \tag{15}$$

Specifying that the distribution functions are step functions, this simplifies to:

$$\begin{aligned}
\langle\langle\rho(x_1,\omega)\rho(x_2,-\omega)\rangle\rangle_{WKB} &= \frac{16e^3V}{\hbar^2\sqrt{v_+(x_1)v_-(x_2)}} \\
& \times \frac{\exp\left[\int_{x_1}^{x_2} i(k'(x) + k(x))dx\right]}{\sqrt{(v'_+(x_1) + v_+(x_1))(v'_-(x_2) + v_-(x_2))}}
\end{aligned} \tag{16}$$

Note the analogy of Eq. (16) with the expressions derived for normal, adiabatic point contact<sup>18</sup>. This illustrates that even for a NS junction with ideal transmission, the decoherence rate does not vanish, as substantial density fluctuations are present, although the current fluctuations are reduced due to the Pauli principle (which operates on electrons and holes on the normal side).

## V. DECOHERENCE RATE AT ARBITRARY BIAS

In the previous expressions, contributions where quasi–particles are transmitted into the superconductor were discarded. Here, the calculation of the density–density correlator proceeds as before, choosing for simplicity zero

temperature, a constraint which excludes some combinations of  $f_{Ne,h}$  and  $f_{Se,h}$ . The calculation proceeds in a similar way as in the Andreev limit, except that processes involving quasi-particle emission from the superconductor now contribute. Operating the simplifications on the wave vectors as before, and using the continuity equation, the density correlator becomes:

$$\begin{aligned} \langle\langle \rho(x_1, \omega) \rho(x_2, -\omega) \rangle\rangle - \langle\langle \rho(x_1, \omega) \rho(x_2, -\omega) \rangle\rangle_A = & \\ \frac{2e^2}{\hbar^2 v_F^2} \int_0^{+eV} d\varepsilon \{ & \\ f_{Ne}(\varepsilon)(1 - f_{Se}(\varepsilon - \omega))\Theta(\varepsilon - \omega) & \\ \times (s'_{NShe} s_{NNhe}^* + s'_{NSee}(e^{-2ik_F x_1} + s_{NNe}^*)) & \\ \times (s_{NShe}^* s_{NNhe} + s_{NSee}^*(e^{2ik_F x_2} + s_{NNe})) & \\ + f_{Ne}(\varepsilon)(1 - f_{Sh}(\varepsilon - \omega))\Theta(\varepsilon - \omega) & \\ \times (s'_{NShh} s_{NNhe}^* - s'_{NSeh}(e^{-2ik_F x_1} + s_{NNe}^*)) & \\ \times (s_{NShh}^* s_{NNhe} - s_{NSeh}^*(e^{2ik_F x_2} + s_{NNe})) & \\ + f_{Ne}(\varepsilon) f_{Se}(-\varepsilon + \omega)\Theta(-\varepsilon + \omega) & \\ \times s_{NSee}^* s_{NNe}^* (s'_{NSee} s_{NNhe} + s_{NShe}(e^{2ik_F x_2} + s'_{NNe})) & \\ + f_{Ne}(\varepsilon) f_{Sh}(-\varepsilon + \omega)\Theta(-\varepsilon + \omega) & \\ \times s_{NSeh}^* s_{NShe}^* (s'_{NSeh} s_{NNhe} + s_{NShh}(e^{2ik_F x_2} + s'_{NNe})) & \} \end{aligned} \quad (17)$$

where  $\langle\langle \rho(x_1, \omega) \rho(x_2, -\omega) \rangle\rangle_A$  is the density-density correlator with Andreev scattering contributions only (yet the energy integral ranges from 0 to  $eV$ , above the gap).

Taking into account that the decoherence rate involves only zero frequency density-density correlations, and that quasi-particle energies are always positive, the decoherence rate reads:

$$\begin{aligned} \frac{1}{\tau_\Phi} - \frac{1}{\tau_\Phi^A} = \frac{e^2}{\hbar^3 v_F^2} \int_0^{eV} d\varepsilon \{ & \\ (s_{NShe} s_{NNhe}^* \tilde{U}(0) & \\ + s_{NSee}(\tilde{U}(-2k_F) + s_{NNe}^* \tilde{U}(0))) & \\ \times (s_{NShe}^* s_{NNhe} \tilde{U}(0) & \\ + s_{NSee}^*(\tilde{U}(2k_F) + s_{NNe} \tilde{U}(0))) & \\ + (s_{NShh} s_{NNhe}^* \tilde{U}(0) & \\ - s_{NSeh}(\tilde{U}(-2k_F) + s_{NNe}^* \tilde{U}(0))) & \\ \times (s_{NShh}^* s_{NNhe} \tilde{U}(0) - & \\ s_{NSeh}^*(\tilde{U}(2k_F) + s_{NNe} \tilde{U}(0))) & \} \end{aligned} \quad (18)$$

In order to enquire about the effect of the oscillatory terms, a Gaussian potential profile with a specific width  $\xi$  is chosen:

$$\begin{aligned} U(x) &= \frac{U_0}{\xi} e^{-\frac{x^2}{2\xi^2}} \\ \tilde{U}(k) &= \frac{U_0}{\sqrt{2\pi}} e^{-\frac{k^2 \xi^2}{2}}, \end{aligned} \quad (19)$$

where  $\xi$  represents the screening length of the Coulomb interaction due to the surrounding metallic gates. For nanoscopic dots and junctions, or alternatively for the large wavelengths which apply to semiconductors-2D electron gas structures, it is becoming conceivable that  $\lambda_F$  could become larger than  $\xi$ .

With this particular choice, the decoherence rate can be expressed as:

$$\begin{aligned} \frac{1}{U_0^2} \left( \frac{1}{\tau_\Phi} - \frac{1}{\tau_\Phi^A} \right) = \frac{e^2}{2\pi \hbar^3 v_F^2} \int_0^{eV} d\varepsilon \{ & \\ (s_{NShe} s_{NNhe}^* + s_{NSee}(e^{-8\pi^2 \frac{\xi^2}{\lambda_F^2}} + s_{NNe}^*)) & \\ \times (s_{NShe}^* s_{NNhe} + s_{NSee}^*(e^{-8\pi^2 \frac{\xi^2}{\lambda_F^2}} + s_{NNe})) & \\ + (s_{NShh} s_{NNhe}^* - s_{NSeh}(e^{-8\pi^2 \frac{\xi^2}{\lambda_F^2}} + s_{NNe}^*)) & \\ \times (s_{NShh}^* s_{NNhe} - s_{NSeh}^*(e^{-8\pi^2 \frac{\xi^2}{\lambda_F^2}} + s_{NNe})) & \} \end{aligned} \quad (20)$$

where the Andreev decoherence rate reads:

$$\begin{aligned} \frac{1}{\tau_\Phi^A U_0^2} = \frac{e^2}{2\pi \hbar^3 v_F^2} \int_0^{eV} d\varepsilon \{ & \\ [s_{NNhe}^* (s_{NNhh} + e^{-8\pi^2 \frac{\xi^2}{\lambda_F^2}}) - s_{NNeh} (s_{NNhe}^* + e^{-8\pi^2 \frac{\xi^2}{\lambda_F^2}})] & \\ \times [s_{NNhe} (s_{NNhh}^* + e^{-8\pi^2 \frac{\xi^2}{\lambda_F^2}}) - s_{NNeh}^* (s_{NNee} + e^{-8\pi^2 \frac{\xi^2}{\lambda_F^2}})] & \} \end{aligned} \quad (21)$$

The results are now illustrated by plotting the decoherence rate as a function of bias voltage, for different values of the potential range  $\xi$ . Because first, it is relevant to enquire about the role of disorder in the NS junction, and second, the complete energy dependence of the scattering matrix coefficients is required, a model with a minimal set of parameters, the BTK model<sup>13</sup>, is chosen. Expressions for the scattering matrix elements of this model are known<sup>8</sup>: there, the same model was chosen to enquire about the singularities in the frequency dependent noise in a NS junction, for arbitrary biases. Recall that the NS junction is described by a delta function barrier  $V(x) = V_B \delta(x)$  and a step-wise pair potential  $\Delta(x) = \Delta \Theta(x)$ , both located at the normal metal-superconductor interface. The strength of the (normal) barrier is represented by the variable  $Z = mV_B/\hbar^2 k_F$ , which for intermediate values between high and low transparencies is of order 1.

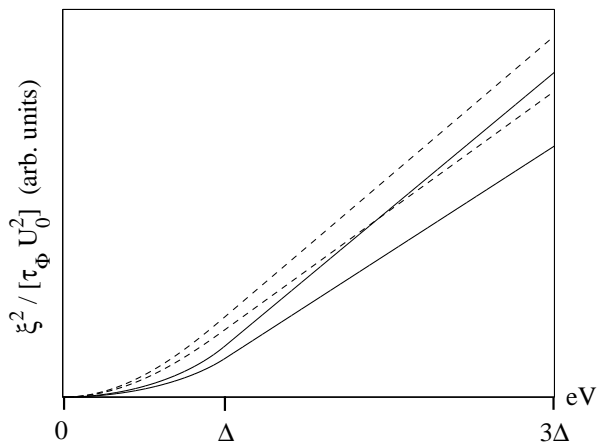


FIG. 2. Decoherence rate  $\xi^2[\tau_\phi U_0^2]^{-1}$  as a function of bias voltage in the Andreev and sub-gap regime, for barrier transparencies:  $Z = 0.1$  (dashed line), at  $\xi = 0.15\lambda_F$  (top) and at  $\xi = 10\lambda_F$  (bottom);  $Z = 1.0$  (full line) at  $\xi = 10\lambda_F$  (top) and at  $\xi = 0.15\lambda_F$  (bottom).

For high to intermediate barrier transparencies, the decoherence rate is plotted in Fig. 2. This rate is normalized to the interaction strength squared  $(U_0/\xi)^2$ , which allows to plot the curves corresponding to  $Z = 0.1$  and  $Z = 1.0$  on the same scale. In addition, results are illustrated for two values of the range  $\xi$  for comparison:  $\xi = 10\lambda_F$  corresponds to a range where the negative exponentials in Eqs. (20) and (21) can be neglected; on the opposite, for  $\xi = 0.15\lambda_F$  these exponentials give a significant contribution.

Deep within the Andreev regime  $eV \ll \Delta$ , the decoherence rate have a linear dependence on the bias (not shown), as the scattering matrix coefficients are essentially energy independent. The rates computed with these parameters show no noticeable change in slope once the voltage bias crosses the gap. This linear dependence is expected for large, sub-gap biases, because transport across the NS junction then becomes dominated by single quasi-particle transfer: similar behavior was recently observed for the finite frequency noise of NS junctions<sup>8</sup>.

It is difficult to predict the behavior of  $\tau_\phi^{-1}$  when the energy dependence of the scattering matrix coefficients becomes noticeable, i.e. for biases near the superconducting gap. In Fig. 2, no qualitative changes of the different decoherence rates are observed until  $eV \sim \Delta$ , above which the rates show a gradual crossover to the linear dependence on the bias. Yet, the results plotted in Fig. 2 show that the relative magnitude of these (normalized) decoherence rates depends in a non trivial manner on the potential range  $\xi$ : for intermediate barriers ( $Z = 1.0$ ) the oscillatory terms in the density-density correlator (Eq. 17) tend to reduce  $\xi^2[\tau_\phi U_0^2]^{-1}$ , while for high transparency barriers, they increase the decoherence rate. In addition, for  $eV \sim 1.9\Delta$  the curves for  $\xi = 10\lambda_F$  corresponding to intermediate and weak barriers cross, and the rate corresponding to  $Z = 1.0$  is larger beyond this.

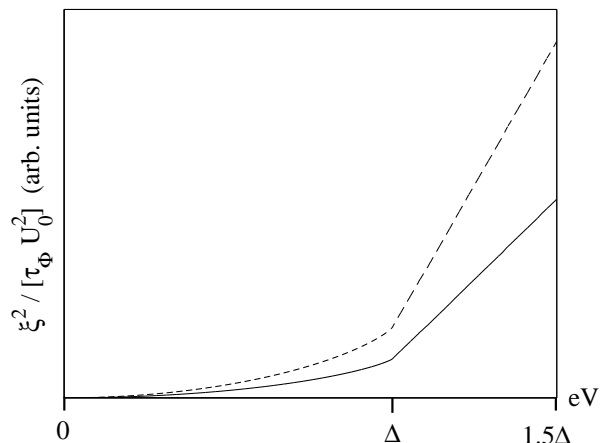


FIG. 3. Same as Fig.2 for opaque barriers ( $Z = 10.$ ):  $\xi = 10\lambda_F$  (dashed line), and  $\xi = 0.15\lambda_F$  (full line).

Most interesting is the behavior of the decoherence rate for opaque barriers ( $Z = 10.$ ), which is illustrated in Fig. 3. For both potential ranges  $\xi = 10\lambda_F$  and  $\xi = 0.15\lambda_F$ ,  $\tau_\phi^{-1}$  displays a clear cusp as the bias crosses the gap. This cusp corresponds to the opening of new scattering channels – electron and hole quasi-particle transfer from the normal metal to the superconductor – which gave previously a gradual change – and no obvious crossover region – for higher transparencies (Fig. 2): here, the crossover region is confined in a very small interval with a width lesser than a few percent of  $\Delta$ . Above the gap, the linear dependence on the bias is recovered.

Note that the decoherence rate should in principle be highest when the current undergoes strong temporal fluctuations: one naively expects<sup>11</sup> that it is related to the shot-noise fluctuations<sup>19</sup>  $\sim T(1-T)$ . Here,  $T$  stands either for the Andreev reflection probability (below the gap) or for the transmission probability of quasi-particles (sub-gap regime). Indeed, the curves corresponding to  $Z = 10$  (Fig. 3) could not be plotted on the same scale as in Fig. 2 because the corresponding rate is too small.

The drastic change depicted in Fig. 3 could possibly be exploited to switch the decoherence rate from “large” to “small”, thus allowing to control the degree of coherence – from quantum to “classical” (phase incoherent) transport – in the neighboring quantum dot (Fig. 1). In addition, note that for existing NS junctions opaque barriers are likely to be the norm rather than the exception, which renders an experimental check of this effect plausible.

## VI. CONCLUSION

The low frequency density-density correlations of a NS point contact have been extracted from the finite frequency noise characteristic, using the continuity equation. This density correlator enters the computation of

the dephasing rate of an isolated quantum system with a discrete spectrum.

In the shot noise regime, the density fluctuation function contains terms which oscillate with half a Fermi wavelength. Because this length scale is considerably larger in semiconductors than in metals, and given the ongoing progress in nano-fabrication techniques, it is suggested that the detection of such oscillations, or their effects in the dephasing rate, could indeed be possible. The role of these oscillatory terms is noticeable for weak disorder even in the (sub-gap) Andreev regime.

Expressions of the density-density correlator described in section IV for a NS junction were generalized to the case of a Superconducting Adiabatic Point Contact, using a semi-classical scheme. Note that this implies that decoherence can even occur when the NS junction located near the quantum dot has ideal charge transmission properties (pure Andreev scattering).

While the computation of the decoherence rate bears similarities with that of a normal-normal point contact<sup>18</sup>, no simple extension so far has been provided when both Cooper pairs and quasi-particles are transmitted in the superconductor. The competition between the two charge transfer processes has been a central issue in the present work.

Regardless of the disorder strength, the decoherence rate rises sharply as the voltage bias is increased above the superconducting gap. Yet for opaque barriers, this transition is even more dramatic, as indicated by the cusp obtained in Fig. 3. This crossover is due to the opening of additional scattering channels, which renders the fluctuating environment more noisy. It is conceivable that this increase of the decoherence rate could have some potential applications.

In particular consider a quantum bit (qubit), implemented by a quantum dot apparatus: the coupling to a neighboring NS junction can render the system classical (besides the tunneling processes in and out of the dot) or quantum in a perfectly controllable manner. Decoherence, reduced abruptly by lowering the voltage bias below the gap, could be used to determine when the quantum evolution of the qubit is supposed to start, or to end. Other applications include the classical resetting of a quantum computer.

The present approach has dealt with a single channel NS wire. Clearly a generalization to a many channel wire would bring this proposal closer to experimental realizations, in carbon nanotubes and so on. Yet, the main goal here has been to demonstrate the variability of the decoherence rate on the bias voltage as it crosses the gap. Because a specific model (BTK) was used to plot the decoherence rate, the additional complexity of dealing with more than one channel could have rendered these results less explicit, but extensions are indeed possible.

Finally, for more immediate experimental applications, it is necessary to work with superconducting materials which have a small enough gap that imposing a voltage bias at the NS junction does not cause substantial heat-

ing on the normal side. Indeed, the present theoretical approach assumes that the transport across the junction is purely elastic, in the mesoscopic regime. Such superconductors with gaps of the order of hundreds of  $mK$  are readily available, and allow presently to observe a crossover behavior in the current noise above and below the gap<sup>20</sup>.

## ACKNOWLEDGMENTS

J. Torres is gratefully acknowledged for help with the BTK scattering matrix elements.

## APPENDIX A: CALCULATION OF THE DECOHERENCE RATE

The starting point for the decoherence rate is the dot Green function:

$$G(t) = -i\langle T[c(t)c^\dagger(0)] \rangle \quad (\text{A1})$$

Operators are in the Heisenberg picture. Specifying the time evolution:

$$\begin{aligned} \langle c(t)c^\dagger(0) \rangle &= \\ &\langle e^{-i\epsilon_0 t/\hbar} T_t e^{-\frac{i}{\hbar} \int_0^t dt' \int dx U(x) \psi^\dagger(x,t) \psi(x,t)} c(0)c^\dagger(0) \rangle \end{aligned} \quad (\text{A2})$$

Following Levinson<sup>10,12</sup>, it is assumed that while the NS point contact has an effect on the dot, the reverse is not taken into account. The Greens function acquires a non-oscillatory time dependence:

$$\langle c(t)c^\dagger(0) \rangle = e^{-i\epsilon_0 t} \exp[-\phi(t)] \quad (\text{A3})$$

where the decoupling between the dot and point contact degrees of freedom allows to compute the average as in a Gaussian process:

$$\begin{aligned} \phi(t) &\simeq -\ln \left[ \langle T_t e^{-\frac{i}{\hbar} \int_0^t dt' \int dx U(x) \psi^\dagger(x,t) \psi(x,t)} \rangle_{NS} \right] \\ &= \frac{1}{\hbar^2} \int_0^t dt' \int_0^t dt'' K(t' - t'') \end{aligned} \quad (\text{A4})$$

The kernel  $K$  is computed assuming that the quantum dot does not perturb the NS point contact:

$$\begin{aligned} K(t) &= \frac{1}{2} \int dx_1 \int dx_2 U(x_1) U(x_2) \\ &\quad \times \langle \langle \rho(x_1, t) \rho(x_2, 0) + \rho(x_2, 0) \rho(x_1, t) \rangle \rangle \end{aligned} \quad (\text{A5})$$

This expression connects the decoherence rate Eq. (3) to the density fluctuations in the superconducting SPC.

The long time behavior of the non oscillatory time dependence in Eq. (A3) is obtained by considering the

density–density kernel. The kernel is characterized by a time scale  $t_c$  which identifies for which times the correlations still survive. Therefore, in the limit  $t \rightarrow \infty$  the second integral over  $t''$  will saturate to a constant :

$$\begin{aligned}\phi(t) &\simeq \frac{1}{2\hbar^2} \int_0^t dt' \int_{-\infty}^{t'} dt'' K(t'') \\ &\simeq \frac{t}{\tau_\phi},\end{aligned}\quad (\text{A6})$$

assuming that for long times, one can replace the second integral over the whole time domain.

## APPENDIX B: FINITE TEMPERATURES

In this appendix, the energy integrals which enter in Eq. (12) are computed analytically.

In the Andreev regime, the elements of the scattering matrix are assumed to be weakly dependent on  $\epsilon$ , so one only needs to compute the integrals of the Fermi Dirac distributions, which have the general form:

$$\begin{aligned}\int_0^{+\infty} d\epsilon \frac{1}{1+e^{\beta(\epsilon \mp eV)}} \frac{1}{1+e^{-\beta(\epsilon - \omega \pm eV)}} = \\ \frac{-1}{\beta(e^{\beta(\omega \mp 2eV)} - 1)} \ln \left\{ \frac{1+e^{\pm\beta eV}}{1+e^{\beta(\omega \mp eV)}} \right\}\end{aligned}\quad (\text{B1})$$

$$\begin{aligned}\int_0^{+\infty} d\epsilon \frac{1}{1+e^{\beta(\epsilon \mp eV)}} \frac{1}{1+e^{\beta(-\epsilon + \omega \pm eV)}} = \\ \frac{-1}{\beta(e^{\beta\omega} - 1)} \ln \left\{ \frac{1+e^{\pm\beta eV}}{1+e^{\beta(\omega \pm eV)}} \right\}\end{aligned}\quad (\text{B2})$$

Combining the thermal factors, the density–density correlator can be computed as :

$$\begin{aligned}\langle\langle \rho(x_1, \omega) \rho(x_2, -\omega) \rangle\rangle &= \frac{2e^2 |s_{eh}|^2}{\hbar^2 \hbar^2 v_F^2} \\ &\left\{ \frac{-4}{\beta(e^{\beta(\omega - 2eV)} - 1)} \ln \left\{ \frac{1+e^{\beta eV}}{1+e^{\beta(\omega - eV)}} \right\} \right. \\ &\quad \times [ |s_{ee}|^2 + s_{ee}^* e^{2ik_F x_2} + s_{ee} e^{-2ik_F x_1} + e^{2ik_F(x_2 - x_1)} ] \\ &+ \frac{4}{\beta(e^{\beta(\omega + 2eV)} - 1)} \ln \left\{ \frac{1+e^{-\beta eV}}{1+e^{\beta(\omega + eV)}} \right\} \\ &\quad \times [ |s_{ee}|^2 + s_{ee}^* e^{2ik_F x_1} + s_{ee} e^{-2ik_F x_2} + e^{2ik_F(x_1 - x_2)} ] \\ &+ \frac{1}{\beta(e^{\beta\omega} - 1)} \ln \left\{ \frac{1+e^{\beta eV}}{1+e^{\beta(\omega + eV)}} \right\} \\ &\quad \times \{ 1 - (|s_{eh}|^2 - s_{ee} s_{hh}) + s_{ee} e^{-2ik_F x_2} + s_{hh} e^{2ik_F x_2} \} \\ &+ \frac{-1}{\beta |s_{eh}|^2 (e^{\beta\omega} - 1)} \ln \left\{ \frac{1+e^{-\beta eV}}{1+e^{\beta(\omega - eV)}} \right\}\end{aligned}$$

$$\begin{aligned}\times \left[ 2 |s_{ee}|^2 \{ |s_{ee}|^2 + 1 + s_{ee} (e^{-2ik_F x_1} + 1/2 e^{-2ik_F x_2}) \right. \\ + s_{ee}^* (e^{2ik_F x_1} + 1/2 e^{2ik_F x_2}) + \cos(2k_F(x_2 - x_1)) \} \\ + s_{ee}^* e^{2ik_F x_2} (1 + s_{ee}^* e^{2ik_F x_1}) \\ \left. + s_{ee} e^{-2ik_F x_2} (1 + s_{ee} e^{-2ik_F x_1}) \right]\end{aligned}\quad (\text{B3})$$

At zero temperature this result corresponds to Eq. (13).

- 
- <sup>1</sup> A. Stern, Y. Aharonov and Y. Imry, Phys. Rev. A **41**, 3436 (1990).
  - <sup>2</sup> A. Yacoby, et al., Phys. Rev. Lett. **74**, 4047 (1995).
  - <sup>3</sup> R. Schuster *et al.*, Nature (London) **385**, 417 (1997).
  - <sup>4</sup> E. Buks *et al.*, Nature (London) **391**, 871 (1998).
  - <sup>5</sup> D. Sprinzak, E. Buks, M. Heiblum and H. Shtrikman, Phys. Rev. Lett. **84**, 5820 (2000).
  - <sup>6</sup> A. A. Kozhevnikov, R. J. Shoelkopf and D. E. Prober, Phys. Rev. Lett. **84**, 3398 (2000).
  - <sup>7</sup> G. B. Lesovik, T. Martin and J. Torrès, Phys. Rev. B **60**, 11935 (1999).
  - <sup>8</sup> J. Torrès, T. Martin and G. B. Lesovik, cond-mat 0004489.
  - <sup>9</sup> A. Martin, T. Gramschpacher and M. Büttiker, Phys. Rev. B **60**, 12 581 (1999).
  - <sup>10</sup> Y. Levinson, EuroPhys. Lett. **39**, 299 (1997).
  - <sup>11</sup> I.L. Aleiner, N.S. Wingreen and Y. Meir, Phys. Rev. Lett. **79**, 3740 (1997).
  - <sup>12</sup> Y. Levinson, Phys. Rev. B **61**, 4 748 (2000) .
  - <sup>13</sup> G. E. Blonder, M. Tinkham and T. M. Klapwijk, Phys. Rev. B **25**, 4515 (1982).
  - <sup>14</sup> M. J. M. de Jong and C. W. J. Beenakker, Phys. Rev. B **49**, 16070 (1994); B. A. Muzykantskii and D. E. Khmel'nitskii, *ibid.* **50**, 3982 (1994); Th. Martin, Phys. Lett. A **220**, 137 (1996) .
  - <sup>15</sup> M. P. Anantram and S. Datta, Phys. Rev. B **53**, 16 390 (1996). Phys. Rev. B **25**, 4515 (1982).
  - <sup>16</sup> N. N. Bogolubov, V. V. Tolmachev and D. V. Shirkov, *A New Method in the Theory of Superconductivity* (Consultant Bureau, New York, 1959); P. G. de Gennes, *Superconductivity of Metals and Alloys*, (Addison Wesley, 1966, 1989).
  - <sup>17</sup> L.I. Glazman, G.B. Lesovik, D.E. Khmel'nitskii, and R.I. Shekhter, JETP Lett. **48**, 239 (1988) (Pis'ma Zh. Eksp. Teor. Fiz. **48**, 218, (1988)).
  - <sup>18</sup> G. Lesovik, JETP Letters **70**, 208 (1999).
  - <sup>19</sup> G. B. Lesovik, JETP Lett. **49**, 592 (1989); M. Büttiker, Phys. Rev. Lett. **65**, 2901 (1990). Th. Martin and R. Landauer, Phys. Rev. B **45**, 1742 (1992).
  - <sup>20</sup> D.C. Glatli and P. Roche, private communication.